International Journal of Greenhouse Gas Control 5 (2011) 138–145

Contents lists available at ScienceDirect

International Journal of Greenhouse Gas Control

journal homepage: www.elsevier.com/locate/ijggc

Laser-based carbon dioxide monitoring instrument testing during a 30-day controlled underground carbon release field experiment

Jamie L. Barr[a], Seth D. Humphries[a], Amin R. Nehrir[a], Kevin S. Repasky[a,*], Laura M. Dobeck[b], John L. Carlsten[c], Lee H. Spangler[b]

[a] Electrical and Computer Engineering Department, Cobleigh Hall Room 610, Montana State University, Bozeman, MT 59717, USA
[b] Chemistry Department, Gaines Hall Room 3400, Montana State University, Bozeman, MT 59717, USA
[c] Physics Department, EPS Room 264, Montana State University, Bozeman, MT 59717, USA

ARTICLE INFO

Article history:
Received 16 October 2008
Received in revised form 19 October 2009
Accepted 14 March 2010
Available online 13 April 2010

Keywords:
Laser diode
Remote sensing
Spectroscopy
Monitoring
Carbon capture

ABSTRACT

The performance of two laser-based instruments for carbon dioxide (CO_2) monitoring was tested during a controlled release experiment performed at the zero emissions research and technology (ZERT) controlled release facility. The first instrument measures path-integrated CO_2 concentrations above ground in two orthogonal directions using a continuous-wave, temperature-tunable, distributed feedback (DFB) diode laser with a center wavelength of 2.003 μm. The second instrument also uses a continuous-wave temperature-tunable DFB laser to deliver light via fiber optics to three underground sensors. Two underground sensors utilize absorption cells of 0.3 and 1 m lengths that are buried 1 m apart approximate 0.75 m above the underground release pipe. The third underground sensor utilizes a photonic bandgap (PBG) fiber as part of a fiber optic sensor. A 0.3 tCO_2/day controlled release was conducted from July 9 to August 7, 2008. The two instruments were able to distinguish the elevated CO_2 concentration associated with the CO_2 injection.

Published by Elsevier Ltd.

1. Introduction

Monthly average atmospheric carbon dioxide (CO_2) concentrations have been measured beginning in 1958 at Mauna Loa and continuing to the present at several sites located around the world (NOAA, 2007). Monitoring sites at the South Pole, Samoa, Christmas Island, Mauna Loa, La Jolla, and Point Barrow all show the same increasing levels of atmospheric CO_2 ranging from a monthly average of 315 parts per million (ppm) in 1958 to a monthly average of 382 ppm in 2007, an increase of 21% (NOAA, 2007). The increase in the atmospheric concentration of CO_2 is largely attributed to the burning of fossil fuels (Masarie and Tans, 1995; Tans, 2006a; Marten Scheffer et al., 2006). Annual CO_2 emissions from burning fossil fuel increased from 23.5 $GtCO_2$/year in the 1990s to 26.4 $GtCO_2$/year from 2000 to 2005 (Keeling et al., 2005). There is growing international concern that the rising levels of atmospheric CO_2 can significantly alter the global climate and environment (Alcamo and Kreileman, 1996; Climate Change, 2001; James Hansen, 2004; Richard et al., 2006; Tans, 2006b; Vinnikov and Grody, 2003; Shackleton, 2000). As a result, international efforts have begun to stem the increase in atmospheric CO_2 concentrations (Tans, 2006a; Alcamo and Kreileman, 1996; Climate Change, 2001; James Hansen, 2004; Richard et al., 2006; Tans, 2006b; Vinnikov and Grody, 2003; Shackleton, 2000).

Carbon sequestration, with an estimated potential storage capacity of 1680 Gt/CO_2, provides one potential solution for curbing CO_2 emission levels (Climate, 2001; Herzog, 2001; IPCCSRCDCS, 2005; LBNL, 2000; Tianfu, 2004; Mingzhe et al., 2006). Geologic carbon sequestration utilizes CO_2 captured at a source such as a coal burning power plant (IPCCSRCDCS, 2005; LBNL, 2000; Tianfu, 2004). The captured CO_2 is compressed and then pumped underground as a supercritical fluid into depleted oil wells for enhanced oil recovery, deep unmineable coal seams, or deep saline formations where the CO_2 is effectively trapped (IPCCSRCDCS, 2005; LBNL, 2000; Tianfu, 2004; Mingzhe et al., 2006).

Initial experimental work in carbon sequestration is underway. Three industrial scale projects currently injecting CO_2 include the Sleipner Saline Aquifer Storage Project (Korbol and Kaddour, 1995), the In Salah Gas Project (This project, in press), and the Weyburn Project (Whittaker et al., 2002; Whittaker, 2004). The Sleipner Saline Aquifer Storage Project is sequestering 1 $MtCO_2$/year in a 200–250 m thick sandstone formation located 800–1000 m beneath the North Sea (Korbol and Kaddour, 1995). The In Salah Gas project began storing 1 $MtCO_2$/year beneath the Algerian desert in a depleted gas field in 2004 (This project, in press). The Weyburn Project is injecting CO_2 into geologic formations for both enhanced oil recovery and CO_2 storage (Whittaker et al., 2002; Whittaker, 2004). The CO_2 used in the Weyburn project is generated in a

* Corresponding author. Tel.: +1 406 994 6082; fax: +1 406 994 4452.
E-mail address: repasky@ece.montana.edu (K.S. Repasky).

1750-5836/$ – see front matter. Published by Elsevier Ltd.
doi:10.1016/j.ijggc.2010.03.002

North Dakota coal gasification facility and is transported through 320 km of pipeline to the Weyburn oil fields (Whittaker et al., 2002; Whittaker, 2004). The North Dakota coal gasification facility generates approximately 6–10 $MtCO_2$/year (Whittaker et al., 2002; Whittaker, 2004). Several smaller scale projects, such as the 100-day injection into a brine formation followed by a year of monitoring and assessment in Frio, Texas (Hovorka et al., 2006), are currently under investigation (IPCCSRCDCS, 2005). In addition, seven Department of Energy (DOE) funded regional partnerships including the Big Sky Carbon Sequestration Partnership, the Plains Regional Carbon Sequestration Partnership, the Illinois Basin Carbon Sequestration Partnership, the Midwest Regional Carbon Sequestration Partnership, the Southeast Regional Carbon Sequestration Partnership, the Southwest Regional Carbon Sequestration Partnership, and the West Coast Regional Carbon Sequestration Partnership are working to develop large volume carbon sequestration tests that will continue to address key issues associated with successful CO_2 storage including site selection, injection monitoring, site closure, and post injection monitoring (Litynski et al., 2008; Benson et al., 2005).

Estimates for successful carbon sequestration require seepage rates to be less than 0.1% of the injection volume per year (Benson et al., 2005). Carbon sequestration site monitoring will require an array of monitoring instrumentation and techniques to ensure the CO_2 remains below ground and to ensure public safety. The Zero Emission Research and Technology (ZERT) Center has developed a field site on the campus of Montana State University (MSU) for testing surface monitoring techniques. This test site allows for a controlled subsurface release of CO_2 using a 100 m long horizontal pipe located below the water table for evaluating monitoring instrumentation and techniques for potential use for measurement, monitoring, and verification of carbon sequestration sites (Humphries et al., 2008).

Two laser-based instruments under development at MSU were tested during a 30-day release conducted at the ZERT controlled release facility from July 9 to August 7, 2008. The first laser-based instrument measured path-integrated above ground CO_2 concentrations continuously over the course of the CO_2 release using a tunable distributed feedback (DFB) laser with a center wavelength of 2.003 μm. The second instrument uses fiber optic cables to deliver the output of a second DFB laser also with a center wavelength of 2.003 μm to three underground sensors. Two underground sensors utilize an open path absorption cell to monitor underground CO_2 levels while the third sensor utilizes a photonic bandgap (PBG) fiber with an open core to measure underground CO_2 concentrations.

This paper is organized as follows. A brief description of the ZERT controlled release facility is presented in Section 2. The laser-based instruments are briefly described in Section 3. Section 4 presents the results and discussion of the controlled CO_2 release experiment. Finally, some brief concluding remarks are presented in Section 5.

2. Controlled release facility

The ZERT (Humphries et al., 2008; Repkasy et al., 2006) controlled CO_2 release facility is located on a 30 acre agricultural plot at the western edge of the MSU-Bozeman campus in Bozeman, Montana. An aerial image of the ZERT facility is shown in Fig. 1. The CO_2 was injected through a 100 m long, 10.16 cm diameter stainless steel pipe with the center 70 m of the pipe slotted. The average depth of the screened section of the horizontal release pipe is 1.8 m below the ground surface putting most of it in the sandy gravel layer and below the water table. Installation of the well screen was done using horizontal directional drilling to minimize the disturbance to the formation.

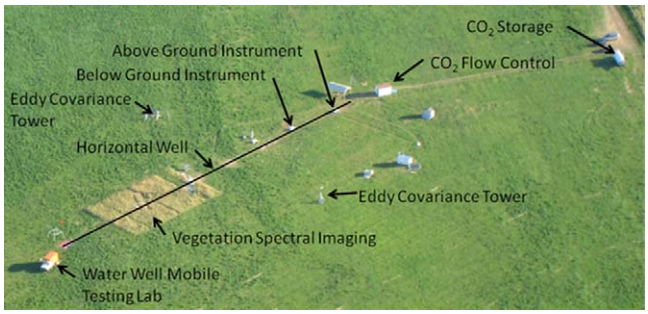

Fig. 1. Aerial photograph of the ZERT CO_2 controlled release facility.

The well is partitioned by a system of packers into six isolated and independent zones. The flow of CO_2 to each zone can be controlled independently and each zone is continuously monitored using dedicated mass flow controllers. In the July 9–August 7, 2008 release, a uniform flow rate was delivered to each of the six zones resulting in a total release of 0.3 tons of CO_2 per day.

The CO_2 flow rate was chosen in the following way. For a 500 MW fossil fuel burning power plant, approximately 4 Mt of CO_2 per year could be captured and sequestered. Over a 50-year period this would results in a total storage of 200 Mt of CO_2. The area of the injection pipe for the ZERT field test is assumed to be approximately 1% of the area of a typical geologic fault. The flow rate was chosen such that a seepage rate of less than 0.01% through the fault would be mimicked. Thus the flow rate was chosen so that the elevated CO_2 levels due to the injection would be approximately at the levels needed for successful monitoring at carbon sequestration sites.

Modeling of the ZERT field site was done to understand how the emitted CO_2 would migrate through the many different soil compositions that make up the field site (Oldenburg et al., 2009). The simulations predicted that the flux is largest directly over the well and falls of rapidly on either side of the well (Oldenburg et al., 2009). The migration of CO_2 was validated by monitoring systems during the 2008 summer field experiment. The distance that the CO_2 traveled away from the well was approximately 1 m at the location of the underground monitoring system. An eddy covariance tower was also tested at the site in order to determine if the total 0.3 tons/day can be accounted for. The eddy covariance tower measured net CO_2 flux with the mean and standard deviation being −12.0 and 28.1 g/(m^2 d) (Lewicki, 2009). The eddy covariance tower calculated the flux at the field as the temporal covariance of CO_2 density and vertical wind velocity, this concept can also be used to convert the CO_2 densities measure by the differential absorption monitoring systems to flux values (Lewicki, 2009; Cuccoli et al., 2007a,b, 2006; Cuccoli and Facheris, 2006; Cardellini, 2003). For the differential absorption instruments considerations for converting measurements to flux values will be made in the future.

3. Instruments

3.1. Above ground sensor

The above ground sensor (Humphries et al., 2008; Repkasy et al., 2006) is based on a tunable DFB laser with a center wavelength of 2.003 μm. The DFB laser is capable of tuning across two water vapor absorption features and four CO_2 absorption features in the 2.0015–2.0042 μm range. The schematic for the above ground instrument is shown in Fig. 3. The output of the DFB laser is collimated with 4% of the outgoing light sent to a reference detector used to monitor the reference power of the DFB laser via a reflection from a wedged pickoff. An extended InGaAs photodiode with a responsivity cutoff of 2.2 μm is used to monitor the reference

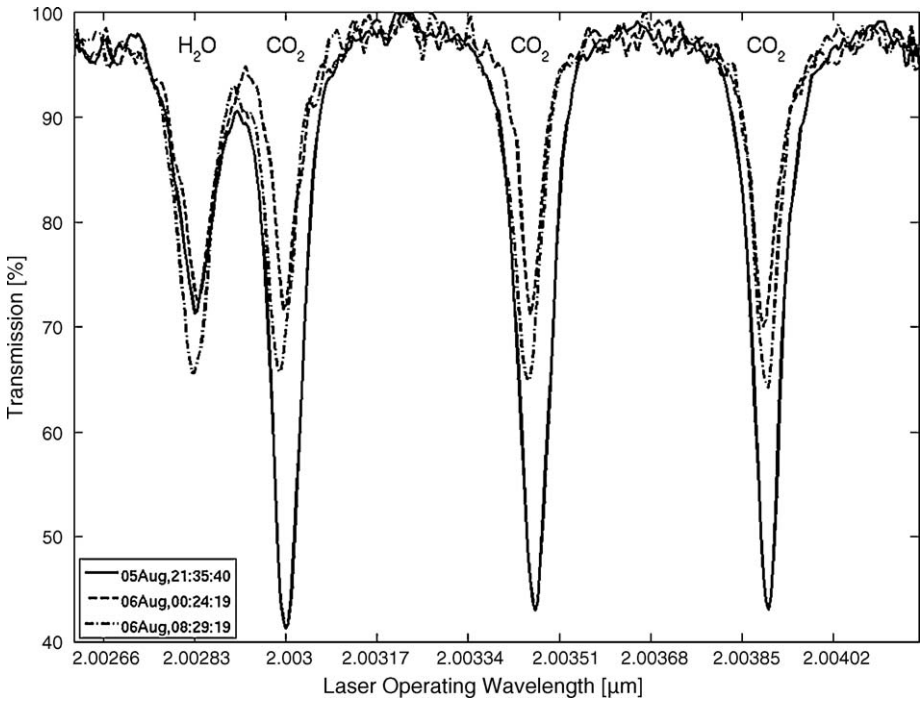

Fig. 2. Normalized transmission as a function of wavelength measured using the above ground instrument. The water vapor and CO_2 absorption features are labeled.

laser power. The light passing through the wedged pickoff is next incident on a mirror that can be moved into or out of the optical beam path by a computer controlled translation stage (Repkasy et al., 2006). With the mirror moved out of the optical beam path (parallel beam path), the light exits the instrument and is incident on a corner cube that directs the light back to the instrument. The light is then sent to another extended InGaAs photodiode which is used to monitor the transmitted optical power. With the mirror moved into the optical beam path (perpendicular optical path), the light exits the instrument perpendicular to the optical path when the mirror is moved out of the optical beam. This light is incident on a second corner cube that directs the light back to the instrument. The light directed back to the instrument is again incident on the moveable mirror that sends the light to the same detector that monitors the optical transmission of the parallel path.

A computer is used to control the wavelength scanning of the above ground sensor in the following manner. The computer sets the temperature of the DFB laser and records both the reference and transmission detector voltages using a data acquisition board. The computer then steps the operating temperature of the DFB laser, which changes the DFB laser's operating wavelength and again reads the reference and transmission detectors. This process is repeated allowing a wavelength scan to be completed across several absorption features. A normalized transmission scan is then calculated by dividing the transmission signal by the reference signal. One scan is recorded with the laser in the parallel optical beam path. The computer moves the mirror into the optical path and again records a tuning scan with the laser in the perpendicular optical beam path. The process is repeated continuously. A plot of the normalized transmission as a function of wavelength is shown in Fig. 2 for several scans taken during the CO_2 release experiment. The normalized transmission is then used along with ambient temperature and pressure measurements taken from a nearby weather station (The Weather, in press) to calculate the CO_2 concentration (Humphries et al., 2008; Rothman et al., 2003). A test using a pressure cell was done to verify the accuracy of the above ground instrument using the process above. The pressure cell measurements indicate that differences in transmission of 1% can be measured with this instrument, indicating that for a 500 m path length for the carbon dioxide absorption line at 2.00402 μm, the instrument can measure carbon dioxide concentration changes of 2.9% (Repkasy et al., 2006).

3.2. Underground sensor

A schematic of the underground sensors is shown in Fig. 4. Light from a temperature-tunable DFB laser with a center wavelength of 2.003 μm is coupled into an FC-APC, single-mode, optical-fiber (SMF-28) (Humphries et al., 2008). An in-line fiber splitter sends approximately half of the light coupled into the optical fiber to box 1 while the remaining light is delivered to box 2. The light delivered to box 1 is again split with an in-line fiber splitter with approximately half of the light coming into box 1 sent to a reference detector D1 and the remaining light launched into a 1 m long

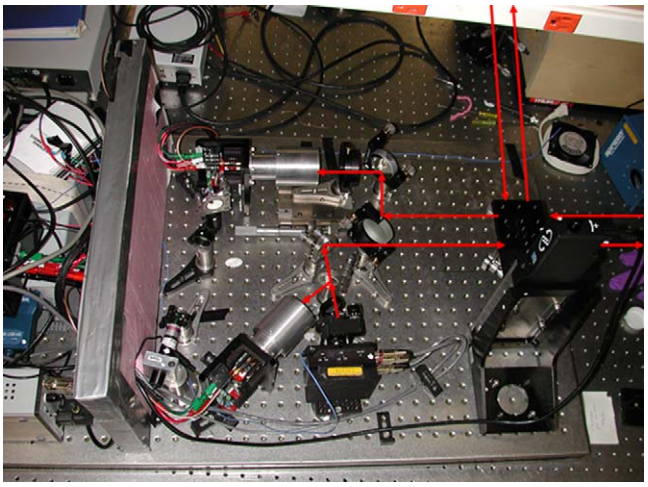

Fig. 3. Picture of the above ground instrument with parallel and perpendicular pathways indicated by the red line. (For interpretation of the references to color in this figure legend, the reader is referred to the web version of the article).

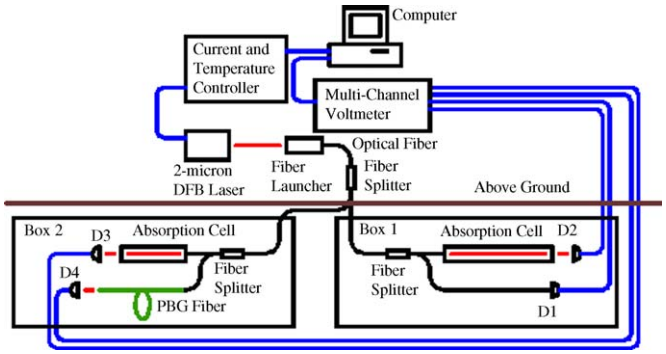

Fig. 4. Schematic of the underground instrument containing the two absorption cell sensors and the fiber optic sensor.

absorption cell. The light transmitted through this absorption cell is monitored using detector D2. The light entering box 2 is split using an in-line fiber splitter with half of the light incident on a 0.3 m long absorption cell. The transmission of the 0.3 m long absorption cell is monitored via detector D3. The remaining light from the fiber splitter is launched into another FC-APC fiber that is fusion spliced to a 1 m long photonic bandgap (PBG) optical fiber with a core diameter of 12 μm (Li et al., 2006; Thapa et al., 2005). The PBG fiber is spliced to a single-mode optical fiber using a fusion splicer (Ericson FSU-995) with a custom program to prevent the hollow core of the PBG optical fiber from collapsing. The output of the hollow core fiber is monitored using a fourth detector D4. Extended InGaAs detectors with a responsivity cutoff of 2.2 μm are used for detectors D1–D4. A picture of the 0.3 m long absorption cell and 1 m long PBG optical fiber sensor housed in the box that is buried underground is shown in Fig. 5. Gas permeable membranes allow the CO_2 to enter the sensors but keeps out water and dirt (FALP, in press). The four detectors are monitored using a multi-channel voltmeter.

The underground sensors utilize a computer to produce spectra in the following way. The computer sets the operating temperature of the DFB laser via a computer controlled current/temperature controller. The four detector voltages are then recorded using a multi-channel voltmeter. The computer then steps the temperature, which changes the operating wavelength of the DFB laser and the process is repeated. Three normalized transmission spectra are then calculated by dividing the voltages read by detectors D2, D3, and D4 by the reference detector voltage read by D1. The normalized transmission spectra are then used to calculate the CO_2 concentrations read by the three sensors. A plot of transmission spectra taken with the 0.3 and 0.1 m absorption cells and the 1 m PBG fiber sensor are shown in Fig. 6. With an accuracy of 1% in measuring transmission the error associated with the underground instrument is at most 0.23%.

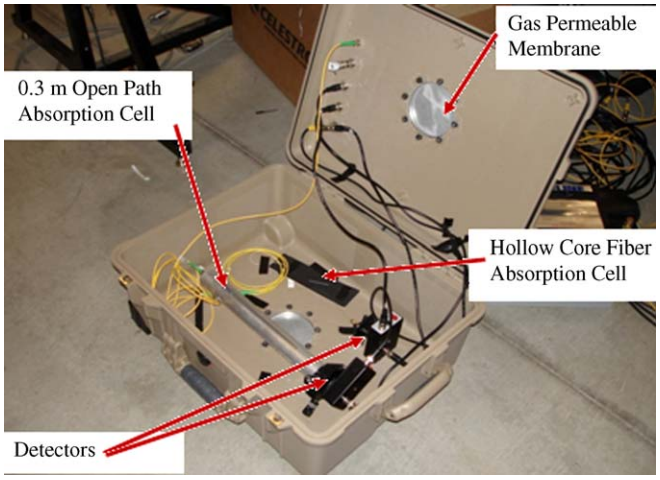

Fig. 5. Picture of the 0.3 m absorption cell and PBG fiber sensor housed in weatherproof box corresponding to box 2 in the schematic shown in Fig. 3. Light from the DFB laser that is housed in a separate weatherproof box located above ground is delivered via an optical fiber to this box which is buried underground.

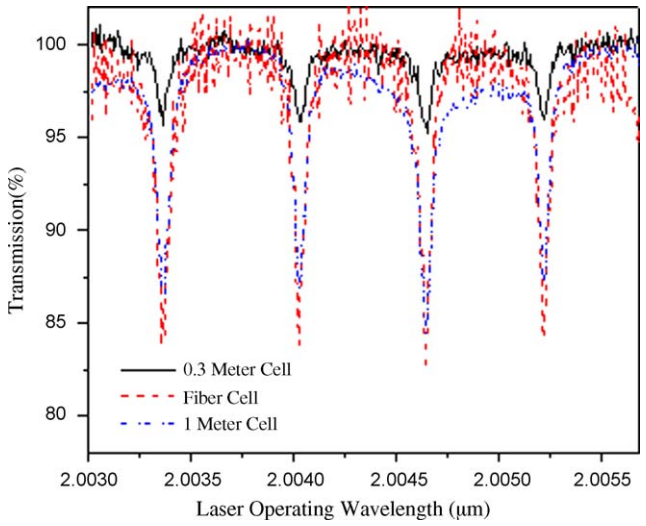

Fig. 6. Normalized transmission as a function of wavelength measured using the below ground instrument. The solid (dashed) line represents measurements made with the 0.3 m (1 m) absorption cell while the dot-dashed line represents measurements made with the PBG fiber sensor.

4. Experimental results

4.1. Above ground sensor results

The above ground sensor was operated continuously from July 1 to August 13, 2008. The above ground sensor was set up with the parallel optical path located directly over and along the direction of the release pipe and the second optical path perpendicular to the release pipe. The corner cube for the optical path located over the pipe was located 29.5 m away from the optical sensor provide a total integrated path length of about 59 m. The corner cube for the optical path perpendicular to the release pipe was located 31 m away from the optical sensor providing a total integrated path length of about 62 m. Both optical beam paths were located at a nominal height of 13 cm above the ground.

A plot of the CO_2 concentration as a function of time measured by the above ground sensor is shown in Fig. 7. The solid line represents measurements made along the direction of the release pipe while the dashed line represents measurements made perpendicular to the release pipe. The beginning and ending of the CO_2 injection are marked as vertical lines on July 9, 2008 and August 7, 2008. Before the injection begins, measurements made parallel to the release pipe and perpendicular to the release pipe have the same values. Once the CO_2 injection starts, measurements made perpendicular to the release pipe are similar to the measurements made before the CO_2 injection, but measurements made parallel to the release pipe increase indicating an elevated CO_2 concentration measured over the release pipe. Approximately 1 day after the CO_2 injection stops, measurements made parallel to the pipe and perpendicular to the pipe have similar values.

One interesting feature seen in both the parallel and perpendicular measurements is the daily cycle of the CO_2 concentration. A plot of the CO_2 concentration as a function of time is shown in Fig. 8 for July 31–August 4, 2008. The CO_2 concentration measure-

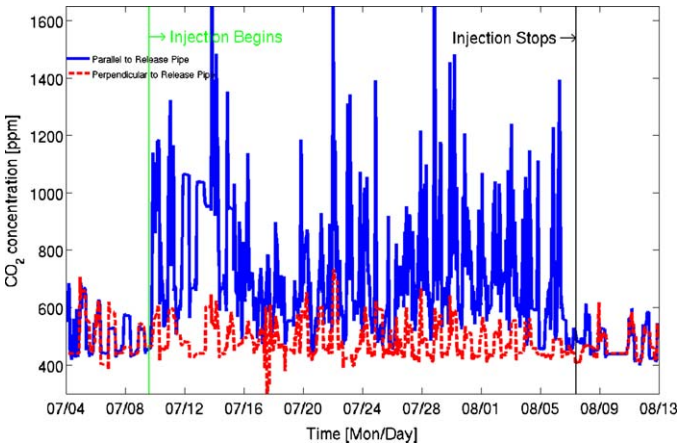

Fig. 7. Plot of CO_2 concentrations measured during the 2008 controlled release by the above ground instrument in the parallel (solid line) and the perpendicular (dashed line) directions relative to the release pipe. The start and end of the injection are designated by vertical lines. The elevated CO_2 levels measured over the release pipe as indicated by the solid line are clearly evident in this figure compared to the background measurements made perpendicular to the release pipe as indicated by the dashed line.

ments made perpendicular to the release pipe show a daily cycle with lower levels of CO_2 measured from mid-morning to mid-evening and higher levels of CO_2 measured from mid-evening to mid-morning. A similar trend is seen for the CO_2 levels measured parallel to the release pipe. Since the elevated CO_2 levels measured over the release pipe result from the CO_2 injection, this diurnal cycle must result from weather conditions including the cooler nighttime temperatures and lower average wind speeds along with CO_2 concentration changes due to photosynthesis.

Above ground monitoring of CO_2 concentrations is affected by weather conditions. To understand how various meteorological conditions can affect the CO_2 concentration measurements, data from a weather station (The Weather, in press) located approximately 300 m north of the release pipe was used. A plot of the CO_2 concentrations as a function of time is plotted as the bottom plot in Fig. 9. The solid line represents measurements made parallel to the release pipe while the dashed line represents measurements made perpendicular to the release pipe. The vertical line just after

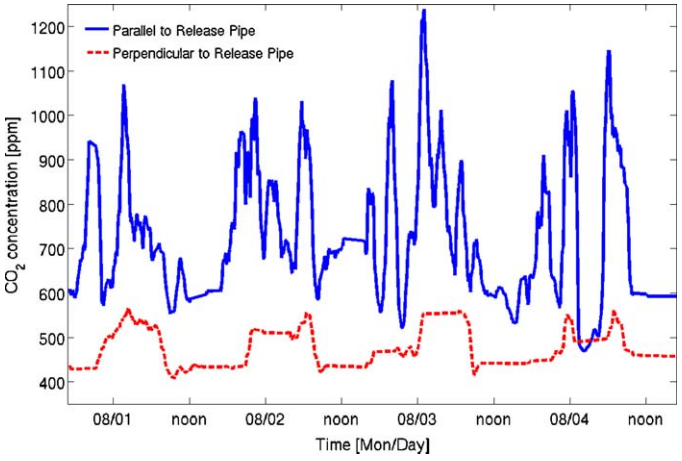

Fig. 8. Plot of CO_2 concentrations measured during the 2008 controlled release by the above ground instrument in the parallel (solid line) and the perpendicular (dashed line) directions from July 31 to August 4, 2008. The diurnal cycle of CO_2 is visible in the data measured perpendicular to the direction of the injection well. A similar diurnal cycle is seen in CO_2 concentrations measured over the release pipe indicating this effect is related to weather conditions including temperature and wind speed as well as natural CO_2 variations due to photosynthesis.

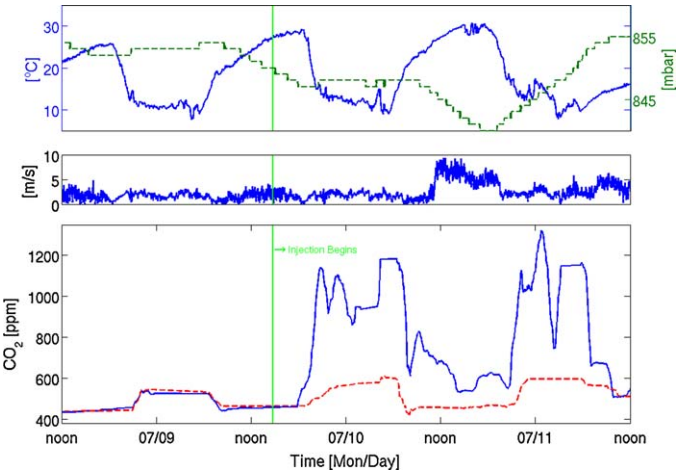

Fig. 9. The bottom plot shows the measured CO_2 concentrations in the parallel (perpendicular) direction indicated by the solid (dashed) line as a function of time. The middle plot shows the measured wind speed measure as a function of time while the top plot shows the temperature (solid line) and absolute barometric pressure (dashed line) as a function of time.

noon on July 9, 2008 indicates the beginning of the CO_2 injection. Wind speed is plotted in the middle plot in Fig. 9. The wind direction is not represented here but can be procured from the weather station present out in the ZERT field site (The Weather, in press). Temperature (solid line) and barometric pressure (dashed line) are plotted as a function of time in the top plot of Fig. 9. On July 10 starting around noon, the wind speed increased corresponding to a decrease in the CO_2 concentration measurement made parallel to the release pipe indicating that increased wind speed causes the CO_2 to disperse. No correlations are apparent between temperature or barometric pressure and CO_2 concentrations for measurements made parallel to the release pipe.

4.2. Below ground absorption cell sensors

The box containing the 1 m long absorption cell and reference detector was buried approximately 0.75 m below the surface at a perpendicular distance of 1 m away from the release pipe. The box containing the 0.3 m absorption cell and PBG fiber was buried approximately 0.75 m below the surface directly over the release pipe. The below ground sensors were operated nearly continuously from July 8 to August 13, 2008. Interruptions to the operation resulted from severe weather events. A plot of the underground CO_2 concentration measurements as a function of time is shown in Fig. 10. The measurements to calculate CO_2 concentrations are made every 8 min while using the third absorption feature to calculate the concentration of CO_2. The solid (dashed) line represents measurements made with the 0.3 m (1 m) absorption cell located over the release pipe (1 m perpendicular distance from the release pipe). Approximately 24 (64) h after the injection starts, the absorption cell located directly over the release pipe (1 m perpendicular distance from the release pipe) begins seeing an increase in the underground CO_2 concentrations. This implies that it takes the CO_2 approximately 40 h to spread a 1 m lateral distance.

Several rain events occurred during the course of the release experiment and were recorded (Rain Data, in press). A plot of the CO_2 concentration as a function of time is shown in Fig. 11 with the solid (dashed) line represents measurements made with the 0.3 m (1 m) absorption cell located over the release pipe (1 m perpendicular distance from the release pipe). Multiple rain events are represented in this plot as vertical bars. These rain events were severe enough to cause an interruption in the electrical power to the field site. The rain events caused the underground CO_2 concentra-

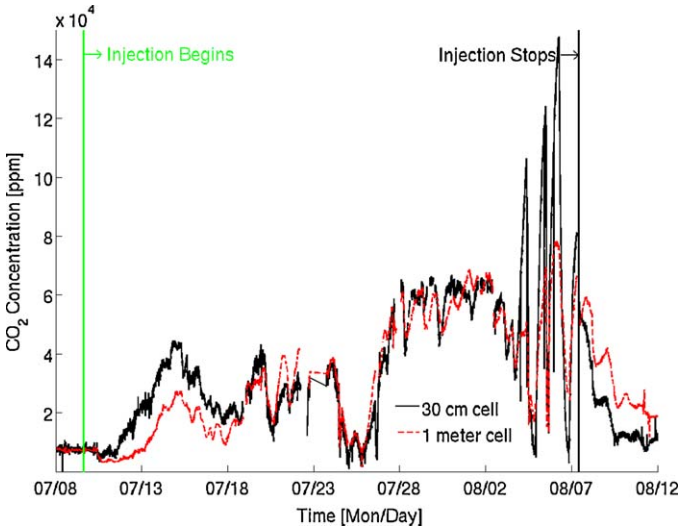

Fig. 10. A plot of the CO_2 concentration measured as a function of time with the underground absorption cells from July 8 to August 12, 2008. The beginning and ending of the CO_2 are indicated by vertical lines. The solid (dashed) line represents measurements made with the 0.3 m (1 m) cell located over (1 m perpendicular distance away from) the injection pipe.

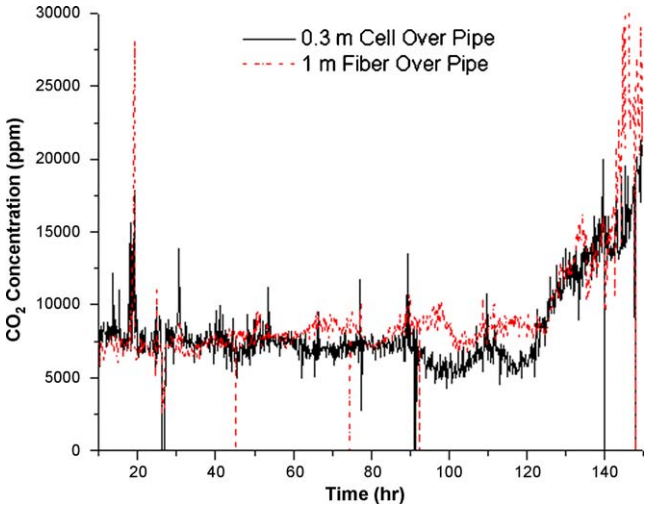

Fig. 12. A plot of the CO_2 concentration measured as a function of time measured using the PBG fiber sensor (solid line) and the co-located 0.3 m absorption cell (dashed line). Good agreement between these two sensors indicated the PBG fiber sensor is a viable option for underground CO_2 monitoring.

tion to drop by either providing pathways for the CO_2 to escape to the surface, forcing the CO_2 down to the water table, or the moisture could change the soil permeability so the CO_2 movement slows.

4.3. Fiber sensor

The underground fiber sensor utilizes a newly available PBG fiber that allows the interaction of the light from the DFB laser source to interact with the CO_2 in the hollow core of the PBG fiber. A plot of the CO_2 concentration as a function of time measured using the PBG fiber sensor is shown in Fig. 12 as the solid line. The concentration measured using the co-located 0.3 m absorption cell is shown as the dashed line in Fig. 12. Laboratory measurements indicate the 1 m length of PBG used for the fiber sensor will lag the absorption cell CO_2 concentrations by approximately 5 h due to the diffusion time associate with the CO_2 into the 12 μm hollow core of the PBG fiber. The agreement between the PBG fiber sensor and the absorption cell measurements indicate that an all optical fiber sensor is capable of monitoring the underground CO_2 concentration levels.

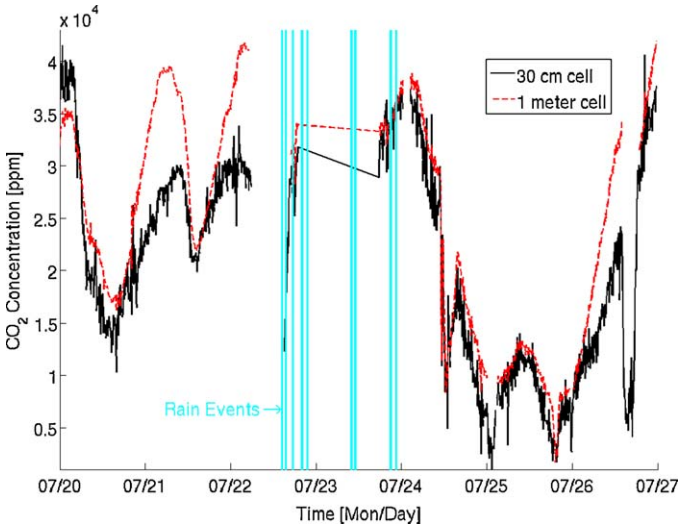

Fig. 11. A plot of the CO_2 concentration measured as a function of time with the underground absorption cells from July 20 to July 27, 2008. The solid (dashed) line represents measurements made with the 0.3 m (1 m) cell located over (1 m perpendicular distance away from) the injection pipe. The vertical lines represent rain events. After rain events, the CO_2 concentrations drop.

4.4. Discussion

Carbon sequestration has the potential to mitigate the climate impacts of increasing atmospheric levels of CO_2 resulting from the use of fossil fuels. Several industry scale CO_2 sequestration projects are underway with regional partnerships planning several more CO_2 sequestration demonstration projects. The ability to monitor carbon sequestration sites is important to ensure the carbon is not released back into the atmosphere and to ensure public safety. This paper presents results from laser-based above ground and below ground monitoring instruments. Each instrument has strengths and weaknesses that need to be considered in terms of a monitoring and verification strategy that will provide adequate coverage on the scales needed for sequestration sites.

The above ground monitoring instrument provides a path-integrated measurement and can provide measurements over paths ranging up to approximately 100 m. Using a scanning mirror, this instrument can provide coverage over approximately 0.01 km^2. While this is a small area compared to the size of a sequestration site, it is much larger than a point measurement. The size of the coverage area is on a scale appropriate for monitoring over faults, abandoned wells, and injection wells. Furthermore, line-of-sight measurements may be useful for pipeline monitoring as well. Three issues that will play a limiting role in laser-based above ground instruments include high wind speeds, rain, and snow coverage. High wind speed causes the CO_2 to disperse making it hard to determine elevated CO_2 levels resulting from seepage compared to background levels. Rain will also affect the ability to monitor CO_2 with above ground instruments by interfering with the beam propagation. However, the effects of high wind speed and rain will only interrupt measurements for brief periods of time and should not pose a problem for longer term monitoring. Snow cover on the ground during the winter months will cause problems with the above ground laser-based monitoring of CO_2 by providing a possible surface layer that can trap the CO_2 thus masking the seepage of CO_2. Snow cover may play a role in interrupting long term above ground monitoring at sites that experience extended snow

coverage such as in the northern United States and Canada. Taking into consideration these facts, it has been concluded that the underground monitoring system would be better suited for future research exploration because fewer environmental factors affecting the system.

The ability of a PBG fiber sensor to measure underground CO_2 concentrations makes possible a relatively inexpensive underground CO_2 monitoring instrument. A single PBG fiber sensor was demonstrated in the controlled release experiment described in this paper. Using a centrally located laser source and a fiber optic switch such as a MEMs based switch allows for a simple design for a multiple point sensor instrument based on an all optical fiber network. The advantages to a network of fiber sensors are the relative low cost and scalability of this instrument. The network of fiber sensors can be deployed along faults, abandoned wells, and injection wells to provide flexible deployment that is best suited for the sequestration site. Using a single laser source and switch at a central location will keep the cost of this network of fiber sensors to a minimum. Using a 2 μm DFB laser diode, where CO_2 has appropriate line strengths associated with its absorption features will allow the use of standard telecommunications fibers such as the SMF-28 fiber. This will further reduce the cost of the instrument. The standard SMF-28 fiber will allow the 2 μm light to propagate approximately 1 km before attenuation becomes a significant problem. This implies that the fiber sensors can cover an area of approximately 1 km^2. The major disadvantage of the network of fiber sensors is related to the fact that the fiber sensor needs to be buried thus making this network of sensors hard to move. Another disadvantage to the underground monitoring system is that in the coldest months of winter ground frost could effect how CO_2 would migrate. As this study has only conducted during the summer further research would be needed to determine the effect ground frost would have on the system.

5. Conclusions

A controlled CO_2 release experiment was performed July 9–August 7, 2008 at the ZERT controlled release facility. A 0.3 tCO_2/day flow rate was maintained over the course of the 30-day release. This paper described the operation of an above ground path-integrated optical sensor that was able to measure the elevated CO_2 levels above the buried release pipe. The elevated CO_2 levels measured during this experiment were clearly visible even with the daily CO_2 cycles. A novel underground fiber optic sensor based on PBG fibers was also demonstrated at this field experiment. The all fiber optic sensor delivers the light from an above ground tunable DFB laser to a PBG fiber with a hollow core. The light interacts with the CO_2 that diffuses into this hollow core allowing the sensor to monitor the below ground CO_2 concentrations. The underground sensors deployed at the controlled CO_2 release experiment were able to measure the elevated CO_2 levels resulting from the controlled underground release.

Acknowledgements

This work was supported by the Department of Energy (DOE) grant number DE-FC26-04NT42262. However, any opinions, findings, conclusions, or recommendations expressed herein are those of the authors and do not necessarily reflect the views of the DOE.

References

Alcamo, J., Kreileman, G.J.J., 1996. Emission scenarios and global climate protection. Global Environmental Change 6 (4), 305–334.

Benson, S.M., Gasperikova, E., Hoversten, G.M., 2005. Monitoring protocols and life-cycle costs for geologic storage of carbon dioxide. In: Proceedings of the 7th International Conference on Greenhouse Gas Control Technologies (GHGT-7), pp. 1259–1266.

Cardellini, C., 2003. Application of stochastic simulation oto CO_2 flux from soil: mapping and quantification of gas release. Applied Geochemistry 18, 45–54.

Climate Change, 2001. Mitigation. The Third Assessment Report of the Intergovernmental Panel on Climate Change. In: Metz, B., Davidson, O., Swart, R., Pan, J. (Eds.), Cambridge University Press, Cambridge, U.K.

Climate Change, 2001. Synthesis Report. A Contribution of Working Groups I, II, and III to the Third Assessment Report of the Intergovernmental Panel on Climate Change. In: R.T. Watson (Ed.), Cambridge University Press, Cambridge, U.K.

Cuccoli, F., Facheris, L., Vaselli, O. 2006. DSA laser measurements and atmospheric diffusion models for the estimation of the gas emission flux by spot source fields: methods and experimental results. Proceedings of SPIE, (6367), 63670K-1–63670K-10.

Cuccoli, F., Facheris, L., 2006. Volumetric gas monitoring through an IR laser network for the control of the gas emission flux by sensitive areas: methods and simulation results. IEEE Internationals 3 (7–11), 907–910.

Cuccoli, F., Facheris, L., Vaselli, O., Tassi, F., 2007a. Five years measurements of CO_2 air concentrations by DSA IR laser devices. Results and perspectives for laser remote sensing systems of gas emissions by critical areas. In: Geoscience and Remote Sensing Symposium, 2007. IEEE International 23–28 July, pp. 4280–4283.

Cuccoli, F., Tassi, F., Vaselli, O., Nisi, B., Montegrossi, G., Longnoli, E., Buccianti, A., Moretti, S., 2007b. Effects on human health and hazard assessment of CO_2-rich gas emissions at Mt. Amiata volcano. In: Proceedings of SECOTOX Conference and International Conference, 24–28 June (1), pp. 283–288.

www.millipore.com catalog number FALP14250.

Herzog, H.J., 2001. What future for carbon capture and sequestration? American Chemical Society 35 (April (7)), 148–153.

Hovorka, S.D., Benson, S.M., Doughty, C., Freifeld, B.M., Sakurai, S., Daley, T.M., Kharaka, Y.K., Holtz, M.H., Trautz, R.C., Nance, H.S., Myer, L.R., Knauss, K.G., 2006. Measuring permanence of CO_2 storage in saline formations: the Frio experiment. Environmental Geosciences 13 (June (2)), 105–121, doi:10.1306/eg.11210505011.

Humphries, S.D., Nehrir, A.R., Keith, C.J., Repasky, K.S., Dobeck, L.M., Carlsten, J.L., Spangler, L.H., 2008. Testing carbon sequestration site monitor instruments using a controlled carbon dioxide release facility. Applied Optics 47 (February (4)), 548–555.

Intergovernmental Panel on Climate Change Special Report on Carbon Dioxide Capture and Storage, 2005. In: Metz, B., Davidson, O., de Coninck, H., Loos, M., Meyer, L. (Eds.), Cambridge University Press, Cambridge, U.K.

James Hansen, 2004. Defusing the global warming time bomb. Scientific American 290 (3), 68.

Keeling, C.D., Piper, S.C., Bacastow, R.B., Wahlen, M., Whorf, T.P., Heimann, M., Meijer, H.A., 2005. Atmospheric CO_2 and $13CO_2$ exchange with the terrestrial biosphere and oceans from 1978 to 2000: observations and carbon cycle implications. A history of atmospheric CO_2 and its effects on Plants. Animals, and Ecosystems, 83–113.

Korbol, R., Kaddour, A., 1995. Sleipner Vest CO_2 disposal-injection of removed CO_2 into the Utsira formation. Energy Conversion and Management 36, 509–512.

Lawrence Berkeley National Laboratory, 2000. An overview of geologic sequestration of CO_2. In: ENERGEX'2000: Proceedings of the 8th International Energy Forum, Las Vegas, NV, July.

Lewicki, J.L., 2009. Eddy covariance observations of surface leakage during shallow subsurface CO_2. eScholarship Repository.

Li, Y., Wang, C., Hu, M., Liu, B., Sun, X., Chai, L., 2006. Photonic bandgap fibers based on a composite honeycomp lattice. IEEE Photonics Technology Letters 18 (January (1)), 262–264.

Litynski, J.T., Plasynski, S., McIlvried, H.G., Mahoney, C., Srivastava, R.D., 2008. The United States Department of Energy's regional carbon sequestration partnerships program validation phase. Environment International 34 (1), 127–138, http://www.sciencedirect.com/science/article/B6V7X-4PYJP9Y-1/2/8e508d282c84843b9faeb5bf15ec81c5.

Marten Scheffer, Victor Brovkin, Cox, P.M., 2006. Positive feedback between global warming and atmospheric CO_2 concentration inferred from past climate change. Geophysical Research Letters 33 (L10702).

Masarie, K.A, Tans, P.P., 1995. Extension and integration of atmospheric carbon dioxide data into a globally consistent measurement record. Journal of Geophysical Research 100 (June), 11593–11610.

Mingzhe, D., Zhaowen, L., Shuliang, L., Huang, S., 2006. CO_2 sequestration in depleted oil and gas reservoirs-caprock characterization and storage capacity. Energy conservation and Management 47, 1372–1382.

Global stations CO_2 concentration trends. Scripps Institute of Oceanography in collaboration with the National Oceanic and Atmospheric Administration (NOAA); November 2007. Available from: http://scrippsco2.ucsd.edu/graphics_gallery/other_stations/global_stations_co2_concentration_trends.html.

Oldenburg, C.M., Lewicki, J.L., Dobeck, L., Spangler, L., 2009. ModelGas transport in the shallow subsurface during the ZERT CO_2 release test. Transport in Porous Media, 11242-009.

Rain data collected by instruments operated by Dr. Jennifer Lewicki of Berkeley National Labs.

Repkasy, K.S., Humphries, S.D., Carlsten, J.L., 2006. Differential absorption measurements of carbon dioxide using a temperature tunable distributed feedback diode laser. Review of Scientific Instruments 77 (11), 113107.

Richard, J., Norby, Yiqi Luo, 2006. Evaluating ecosystem responses to rising atmospheric CO_2 and global warming in a multi-factor world. New Phytologist 162 (2), 281–293.

Rothman, L.S., Barbe, A., Chris Benner, D., Brown, L.R., Camy-Peyret, C., Carleer, M.R., Chance, K., Clerbaux, C., Dana, V., Devi, V.M., Fayt, A., Flaud, J.-M., Gamache, R.R., Goldman, A., Jacquemart, D., Jucks, K.W., Lafferty, W.J., Mandin, J.-Y., Massie, S.T., Nemtchinov, V., Newnham, D.A., Perrin, A., Rinsland, C.P., Schroeder, J., Smith, K.M., Smith, M.A.H., Tang, K., Toth, R.A., Vander Auwera, J., Varanasi, P., Yoshino, K., 2003. The HITRAN molecular spectroscopic database: edition of 2000 including updates through 2001. Journal of Quantitative Spectroscopy & Radiative Transfer 82 (March), 5–44.

Shackleton, N.J., 2000. The 100,000-year ice-age cycle identified and found to lag temperature, carbon dioxide, and orbital eccentricity. Science 289 (September), 1897–1902.

Tans, P.P., 2006a. How can global warming be traced to CO_2? Scientific American 295 (December (6)), 124.

Tans, P.T., 2006. Trends in atmospheric carbon dioxide. National Oceanic & Atmospheric Administration, 17, April.

Thapa, R., Knabe, K., Corwin, K.L., Washburn, B.R., 2005. Arc fusion splicing of hollow-core photonic bandgap fibers for gas-filled fiber cells. Optics Express 14 (21), 9576–9583.

The weather station is operated and maintained by Dr. Joe Shaw and Nick Jurich. Data is publicly available at http://www.coe.montana.edu/ee/weather/zert/.

This project is described at http://www.bp.com.

Tianfu, Xu, 2004. CO_2 geological sequestration. Lawrence Berkeley National Laboratory. Paper LBNL-56644 JArt, November 18.

Vinnikov, K.Y., Grody, N.C., 2003. Global warming trend of mean tropospheric temperature observed by satellites. Science 302 (October), 269–272.

Whittaker, S.G., 2004. Geological storage of greenhouse gases: the IEA Weyburn CO_2 monitoring and storage project. Canadian Society of Petroleum and Geologists Reservoir 31 (September (8)), 9.

Whittaker, S.G., Kreis, K., Davis, T.L., Hajnal, Z., Heck, T., Penner, L., Qing, H., Rostron, B., 2002. Characterizing the geologic container at the Weyburn Field for subsurface CO_2 storage associated with enhanced oil recovery. In: Proceedings of the Diamond Jubilee convention of the Canadian Society of Petroleum Geologists.